

## MODELING OF THE PENETRATION OF A SUPERCRITICAL MAGNETIC FIELD INTO A TYPE II SUPERCONDUCTOR AND THE ELECTROMAGNETIC RADIATION GENERATED THEREBY

A. B. Prischepenko,<sup>1</sup> A. A. Barmin,<sup>2</sup> and O. É Mel'nik<sup>2</sup>

UDC 537.872.3

Traditional superhigh-frequency (SHF) vacuum electronic devices show rather limited possibilities of extending the spectrum of the generated-radiation (usually, marked power levels are observed at frequencies that differ from the main frequency by not more than 10–20%). The frequency range of the generated SHF radiation can be extended only using a fundamentally new element basis, commutating high-speed elements playing a primary role.

In the present paper, we consider the physical principles of operation of a superwide-band radiation source which uses a type II superconductor — an annular layer of  $\text{YBa}_2\text{Cu}_3\text{O}_7$  ceramic. Most of the electromagnetic radiation is generated when a magnetic field emerges from the superconductor.

This process is described using the generalized London brothers equations [1], but, in contrast to the classical theory, it is assumed that the number of superconducting electrons is not constant but depends on the magnetic field and temperature. This dependence is obtained from the experimental data of [2]. The proposed model is used to analyze numerically the penetration of a magnetic field into a hollow cylindrical superconductor, the propagation of the zone of loss of superconducting properties, and the emergence of the field from the superconductor. The power and spectrum of the generated electromagnetic radiation are estimated from the current distribution in the superconductor using the theory of a wave oscillator [3]. The results obtained are compared with the experiment.

**1. Formulation of the Problem.** As an external magnetic field reaches a critical magnitude  $B^*$ , it penetrates almost instantaneously into type I superconductors, among which are almost all pure metals (the thickness of the transient region is of the order of  $L_0$  — the characteristic dimension of the Cooper pair).

Modern high-temperature superconductors are among type II superconductors. A magnetic field penetrates gradually into them (there is a region with width  $\delta$  in which a magnetic field exists). When  $\delta/L_0 \gg 1$ , the theory of [1] gives the penetration depth  $\lambda_L = \sqrt{mc^2/(4\pi ne^2)}$ , where  $m$ ,  $e$ , and  $n$  are the electron mass, charge, and density. It is assumed in this theory that all electrons are in a superconducting state. In reality, along with superconducting electrons with concentration  $n_s$ , normal electrons are also present in the transient region. The closer the magnetic-field intensity or the temperature to their critical values, the higher the concentration of the normal electrons  $n_n$ . Thus, the electric current can be regarded as two parallel currents due to superconducting and normal electrons. In this case, the generalized London brothers equations [1] has the form

$$\begin{aligned} \frac{\partial \mathbf{B}}{\partial t} + c \operatorname{rot} \mathbf{E} = 0, \quad \mathbf{j} = \frac{c}{4\pi} \operatorname{rot} \mathbf{B}, \quad \mathbf{j} = \mathbf{j}_n + \mathbf{j}_s, \quad m \frac{\partial \mathbf{V}_s}{\partial t} = e \mathbf{E}, \\ \mathbf{j}_s = \alpha n \mathbf{V}_s, \quad \mathbf{j}_n = \sigma_0 (1 - \alpha) \mathbf{E}, \quad \alpha = n_s/n. \end{aligned} \quad (1.1)$$

Here  $\mathbf{B}$  and  $\mathbf{E}$  are the intensities of the magnetic and electric fields,  $\mathbf{j}$  is the current density;  $\mathbf{V}_s$  is the velocity of superconducting electrons; the subscripts  $n$  and  $s$  refer to the normal and superconducting states,

---

<sup>1</sup>Central Scientific Research Institute of Chemistry and Mechanics, Moscow 115487. <sup>2</sup>Institute of Mechanics, Moscow State University, Moscow 119899. Translated from *Prikladnaya Mekhanika i Tekhnicheskaya Fizika*, Vol. 38, No. 3, pp. 3–9, May–June, 1997. Original article submitted February 12, 1996.

respectively. Relations (1.1) represent the Maxwell equations, the condition of parallel currents, and Ohm's laws for normal and superconducting electrons.

To close system (1.1), it is necessary to specify the dependence  $\alpha = \alpha(B, T)$ . The dependence of the resistivity  $\rho$  of superconductor  $\text{YBa}_2\text{Cu}_3\text{O}_7$  on the magnitude of magnetic field for various temperatures lower than the critical temperature is given in [2]. Assuming that  $\rho(B, T) = (1 - \alpha(B, T))\rho_0$  we obtain  $\alpha = 1 - \rho(B, T)/\rho_0$  ( $\rho_0 = 0.3 \text{ m}\Omega \cdot \text{cm}$ ). A characteristic feature of type II superconductors is the existence of two critical fields; the lower  $B_1^*$  and the upper  $B_2^*$  fields. If the magnetic-field intensity is lower than the lower critical value, the material behaves as a pure superconductor, which corresponds to  $\alpha = 1$ . If the field is higher than the upper critical field, we have  $\alpha = 0$ , and the material is a normal conductor. In the transient region, the dependence  $\alpha(B)$  is well approximated by the formula

$$\alpha = \frac{a_1 + a_2(B - b) - (a_2 + 1)(B - b)^2}{a_1 + a_2(B - b) - a_3(B - b)^2},$$

where  $B$  is the ratio of the magnetic-field intensity to the upper critical value,  $b$  is the dimensionless critical field, and the parameters  $a_i$  are determined by the body temperature.

To estimate the possible increase in temperature caused by Joule heating of the superconductor, we use the energy-balance equation. Ignoring heat-conduction processes (which are much slower), we write this equation as

$$\rho c \frac{\partial T}{\partial t} = \sigma_0(1 - \alpha)\mathbf{E}^2. \quad (1.2)$$

In the calculations, we shall estimate the temperature variation from currents.

We consider the following one-dimensional problem. Let a superconductor be an infinite hollow cylinder with outside radius  $r_e$  and inside radius  $r_i$ . We assume that the distribution of electromagnetic fields inside the cylinder is described by the Maxwell equations for vacuum, and, inside the cylinder, it is described by Eq. (1.1). A magnetic field  $B = B(t)$  parallel to the cylinder axis is specified at the external boundary of the cylinder. At the initial time, the field was absent:  $B(r, 0) = 0$  ( $0 \leq r \leq r_e$ ). For  $r = r_i$ , we assume continuity of the electric and magnetic fields, which corresponds to the absence of surface currents and charges, and, for  $r = 0$ , the fields are considered finite.

The problem reduces to integration of two systems of one-dimensional nonstationary equations in partial derivatives, conjugated at the motionless boundary  $r = r_i$  by the field-continuity condition. System (1.1) is parabolic, and the Maxwell equations for vacuum are hyperbolic.

The problem was solved numerically. The conservative scheme of [4] was used to write only nonexplicit difference analogs of the system. Then, matrix coefficients were processed in the directions from the boundaries to  $r = 0$  and  $r = r_e$ , and the magnitudes of fields at the external boundary of the superconductor were determined from these coefficients and the boundary conditions at  $r = r_i$ . Finally, the distribution over the entire calculation domain was found by inverse processing. The accuracy of the difference approximation is of order  $[\tau, h^2]$ , and the scheme is absolutely stable in this case.

To characterize the penetration of the field into the superconductor, we introduce the quantities  $\lambda_1 = r(B_1^*)$  and  $\lambda_2 = r(B_2^*)$  ( $r$  is the distance from the boundary of the superconductor), and also the mean value of field penetration  $\lambda$

$$\Lambda \equiv \lambda(r_0 - (1/2)\lambda)B_0 = \int_{r_1}^{r_e} B(r)r dr.$$

Using system (1.1) when  $B_0 < 1$ , for  $\Lambda$  we obtain

$$\Lambda(t) = e^{-t} \int_{\tau_0}^t \frac{1}{\alpha_0} \left( \frac{\partial B}{\partial x} \right)_0 d\tau, \quad \tau - \tau_0 = \int_0^t \frac{\alpha}{1 - \alpha} dt. \quad (1.3)$$

Here the subscript zero refers to the value at the boundary of the superconductor ( $r = r_e$ ). As  $t \rightarrow \infty$ , we have  $d\lambda/dt \rightarrow 0$ , and, hence, there is a limiting profile which is nearly exponential at large distances from the

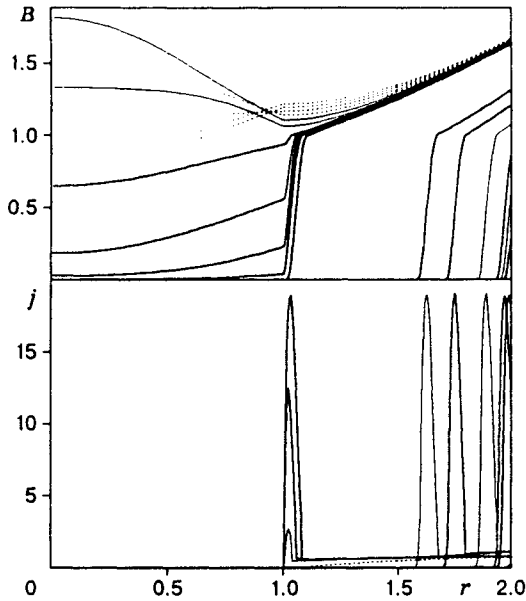


Fig. 1

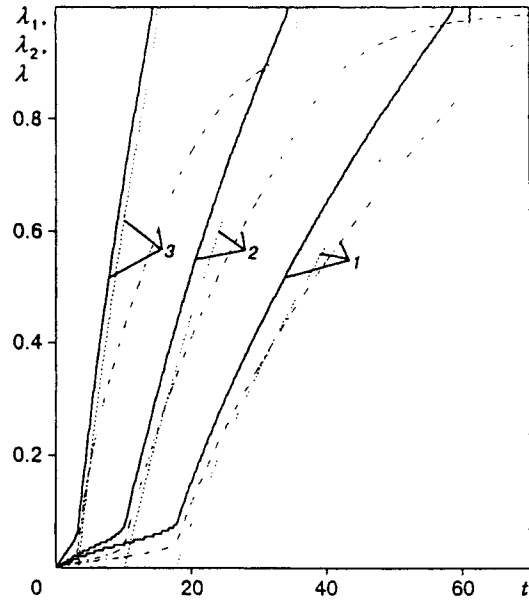


Fig. 2

boundary. According to (1.3), the function  $\lambda$  is finite and increases with increase in  $B_0$ .

**2. Penetration of a Magnetic Field into the Superconductor.** We study the penetration of a magnetic field into the hollow cylindrical superconductor as a function of the applied magnetic field at the boundary  $B_0$  and its variation. If  $B_0 > B_2^*$ , the following three regions are formed:

- I — the superconducting region ( $r > \lambda_1$ ),
- II — the region of mixed conduction ( $\lambda_1 > r > \lambda_2$ ),
- III — the region of normal electrical conduction.

The quantity  $\lambda$  increases continuously. For  $B_0 = B_2^*$ , we have  $\lambda \approx \ln t$  and, for  $B_0 > B_2^*$ , we have  $\lambda \approx t^{\gamma(B_0)}$ , and  $\gamma \rightarrow 0.5$  with increase in  $B_0$ . This shows that the determining process is the field penetration into the region of normal conduction, in which the process is described by the ordinary heat conduction equation.

As the law of variation of the field at the external boundary of the cylinder, we assume  $B(r_e, t) = (2/\pi)B_0 \arctan(\omega t)$ .

The quantity  $\omega = \infty$  corresponds to instantaneous specification of the maximum magnitude of field. Here and below, dimensionless quantities are used unless dimension is indicated explicitly. The magnetic-field intensity is divided by the upper critical value, i.e.,  $B_2^* = 1$ , the time is divided by  $r_i/c$ , the distance for  $r_i \leq r \leq r_e$ , including  $\lambda_1$ ,  $\lambda_2$ , and  $\lambda$ , is divided by  $\Delta r = r_i - r_e$ , and, for  $r < r_i$ , i.e., for vacuum, it is divided by  $r_i$ , the current density is divided by  $B_2^*c/\Delta r$ , and the magnetic moment of the system of currents is divided by  $B_2^*c/\Delta r^4$ .

Figure 1 gives magnetic-field and current-density profiles for  $\omega = 0.1$  for  $B_0 = 2$  (the dashed curves show the profiles after reflection of the wave from the center). Here, for  $0 < r < 1$ , we have vacuum, and, for  $1 \leq r \leq 2$ , we have the conducting material. As long as  $B(r_e, t) < 1$ , the value of  $\lambda_1$  is of the order of several London length and increases slowly with increase in field, and the current flows in a narrow region near the boundary. As soon as  $B(r_e, t) > 1$ , the penetration depth increases suddenly, and the three regions indicated above are formed. The main current flows in region II, which can be regarded as the wave due to loss of superconductivity. In region III, the current decays rapidly because of ohmic losses. The estimate obtained by Eq. (1.2) shows that a considerable increase in temperature occurs only in region III, and does not markedly affect the transition from the superconducting to the normal state.

The curves of  $\lambda_1(t)$ ,  $\lambda_2(t)$  and  $\lambda$  (the solid, dashed, and dot-and-dashed curves, respectively) for  $\omega = 0.1$

TABLE 1

$B_0$	$\omega$							
	0.05		0.1		1.0		$\infty$	
	$t_1$	$t_2$	$t_1$	$t_2$	$t_1$	$t_2$	$t_1$	$t_2$
	nsec							
1.5	34.7	89.7	17.4	61.1	1.7	28.2	0	21.6
2	20.0	52.6	10.0	35.8	1.0	16.2	0	12.2
5	6.5	21.3	3.3	14.8	0.4	6.7	0	4.8

TABLE 2

$B_0$	$\omega$			
	0.05	0.1	1.0	$\infty$
	$S, \text{ MW}$			
1.5	0.26	0.27	0.31	0.33
2	0.76	0.85	0.92	1.03
5	2.77	4.21	8.93	9.32

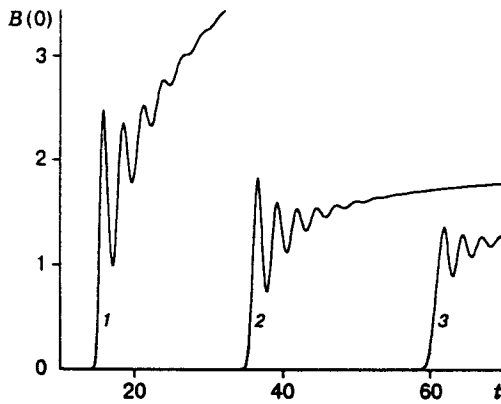


Fig. 3

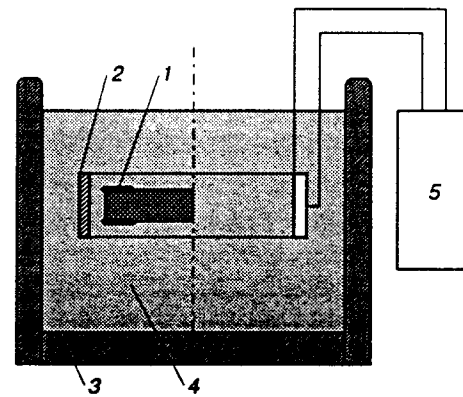


Fig. 4

$B_0 = 1.5, 2,$  and  $5$  are given in Fig. 2 (curves 1–3). With increase in  $B_0$ , the time of loss of superconductivity in the cylindrical layer increases due to both the later attainment of the value  $B = 1$  at the boundary and increase in  $d\lambda_i/dt$ . The width of the region of mixed conduction increases in this case. A decrease in  $\omega$  leads to similar results.

In the initial region, the field-penetration depth changes primarily because of the propagation of the wave due to loss of superconductivity. As the front reaches the boundary of the conducting material, the penetration depth is determined by normal conductivity.

Table 1 gives the times of loss of superconductivity in the ring considered versus the rate of increase in intensity at the field boundary and versus the maximum magnitude of the field. The times  $t_1$  and  $t_2$  correspond to the attainment of the upper critical field at the internal and external boundary of the superconductor, respectively.

When region II disappears, the magnetic-field intensity at the internal boundary increases suddenly to the value  $\sim B_2^*$ . This change in field propagates in the nonconducting region as electromagnetic waves reflected from the center of the conducting cylinder. In the chosen geometry, the time of the sudden change in field at the boundary is equal to 2–3 units of dimensionless time.

Figure 3 shows the variation in intensity at the center  $B(0)$  versus  $t$  for  $\omega = 0.1$  and  $B_0 = 5, 2,$  and  $1.5$  (curves 1–3). The initial fluctuations are induced by wave reflection, and then the field approaches asymptotically the applied external field  $B_0$ . The maximum value in the first peak exceeds  $B(r_i)$  by a factor of 1.5–3, depending on  $\omega$ , and can be smaller than  $B_0$ . The latter is caused by the delayed penetration of the field through the conducting layer. Hence, strong compression of the field is impossible because of the loss of superconductivity.

**3. Superwide-Band Source of SHF Radiation.** The calculations performed were used to explain the principles of operation of an SHF radiation source with a continuous frequency spectrum covering

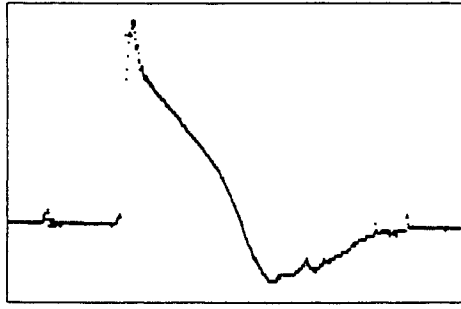


Fig. 5

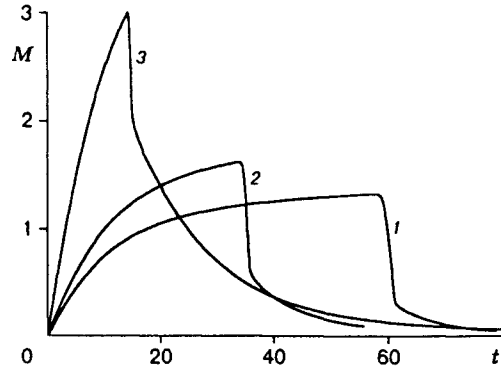


Fig. 6

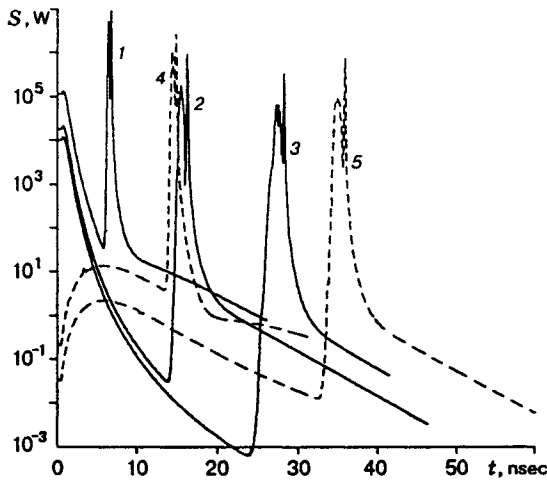


Fig. 7

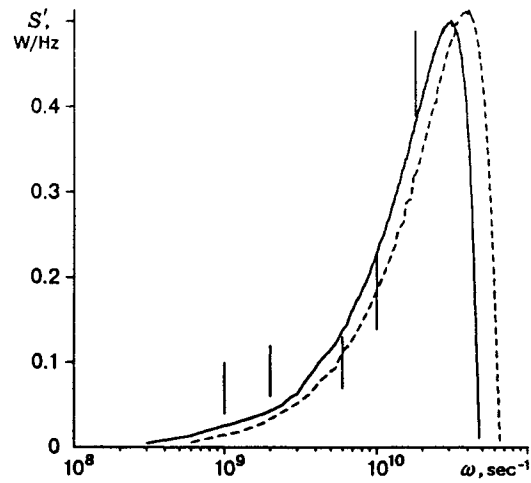


Fig. 8

frequencies from fractions to tens of gigahertz.

The source developed by A. B. Prischepenko is shown schematically in Fig. 4, where 1 is the annular layer of superconducting  $\text{YBa}_2\text{Cu}_3\text{O}_7$  ceramic, 2 is the coil producing a pulsed magnetic field, 3 is the heat-insulated cuvette, 4 is liquid nitrogen, and 5 is the pulsed electric current generator. An oscillogram of the coil current is shown in Fig. 5. The time distance between points is 50 nsec, and the maximum amplitude is 25 kA. The change in magnetic field inside the coil is proportional to the current.

The moment of current in the superconductor is of importance for an understanding of the radiation mechanism. For a unit length of the cylindrical specimen, it can be written as

$$M(t) = \int_{r_i}^{r_0} r^2 \frac{\partial B}{\partial r} dr = (r_0 - \lambda)^2 B(r_e) - r_i^2 B(r_i).$$

Figure 6 shows the variation in the moment of current  $M$  versus time  $t$  for  $\omega = 0.1$  and  $B_0 = 1.5, 2,$  and  $5$  (curves 1—3). In the initial stage,  $M$  increases due to change in  $B_e$ , since the value  $\lambda/r_0$  is small, and  $B(r_i) = 0$ . When region II reaches  $r_i$ , the second term begins to grow rapidly, leading to an abrupt drop in  $M(t)$ .

Specifically, this drop is determined primarily by the rate of change of  $B_i$ , which, as noted above, depends only slightly on the rate of change of field at the external boundary. After complete loss of superconductivity, the processes are determined by the usual diffusion, and the change of  $M(t)$  is suddenly decelerated. Note that  $M''(t)$  changes sign. Such behavior of  $M(t)$  explains why this system is an effective

radiator of electromagnetic waves.

To estimate the power, we calculated the resulting electromagnetic radiation as the emission of a magnetic dipole with specified magnetic moment [3]. Plots of the radiation power  $S(t)$  are given in Fig. 7 for  $\omega = 1$  and  $B_0 = 5, 2,$  and  $1.5$  (curves 1-3) and for  $\omega = 0.1$  and  $B_0 = 5$  and  $2$  (curves 4 and 5).

The maximum radiation power decreases with decrease in  $B_0$ , and the rate of increase in the external field  $\omega$  has a weaker effect (see curves 1 and 4 in Fig. 7 and Table 2). The drop in the radiation peak corresponds to the change of sign of  $M''(t)$ . The duration of the main radiation pulse is  $\approx 0.8$  nsec for  $B_0 = 5$  and  $2.7$  nsec for  $B_0 = 1.5$ . It increases with decrease in  $B_0$ , and this is associated with a decrease in the current-wave velocity. The radiation caused by increase in the external field is determined by the rate of its change, and, for the processes considered, it is several orders smaller than the maximum. Thus, for  $\omega = 1$  and  $B_0 = 5$  (curve 1), it amounts to 1% of the main maximum.

Table 2 gives values of the maximum radiation power  $S$  for the variants considered above. For the case of  $\omega = \infty$ , the given value corresponds to the emergence of a current wave from the conductor. The more stronger dependence of the radiation power on  $\omega$  for  $B_0 = 5$  is due to the fact that, at the moment the current wave emerges from the superconductor and enters vacuum, the magnitude of the field at its external boundary is the larger, the greater  $\omega$ .

The calculations performed suggest that the radiation generated by an annular superconducting commutator is caused by the sudden change in its magnetic moment with the loss of superconductivity over the entire volume of the superconductor.

The proposed radiation mechanism is supported by a comparison of the calculated spectrum with the experimental one obtained using the setup described above. The spectral radiation power  $S'$  was measured by means of a four-channel spectrometer with transmission bands of 70 MHz for each of the channels, produced in the laboratory. The resolution time of peak detectors is 10 nsec. The measurement accuracy is estimated at  $\pm 25\%$ .

Figure 8 shows the radiation spectrum for  $\omega = 0.1$  and  $B_0 = 2$  and  $5$  (solid and dashed curves). The agreement between the calculation and experimental data (vertical bars) is satisfactory if one takes into account the model character of the calculation scheme. The frequency range is shifted to higher values of  $\omega$  with increase in  $B_0$ .

Thus, the electromagnetic radiation observed experimentally with loss of superconductivity under the action of a pulse of the magnetic field in a superwide-band SHF radiation source is explained on the basis of a phenomenological model that is an extension of the London theory with allowance for the experimental dependence of superconducting electrons on magnetic-field intensity.

## REFERENCES

1. A. Rose-Innes and E. Roderick, *Introduction to the Physics of Superconductivity* [Russian translation], Mir, Moscow (1972).
2. D. M. Ginzburg (ed.), *Physical Properties of High-Temperature Superconductors* [in Russian], Mir, Moscow (1990).
3. I. E. Tamm, *Foundations of Electricity Theory* [in Russian], Nauka, Moscow (1984).
4. V. L. Ginzburg and D. A. Kirzhnits (eds.), *Problems of High-Temperature Superconductivity* [in Russian], Nauka, Moscow (1977).
5. A. A. Samarskii and Yu. P. Popov, *Difference Schemes of Gas Dynamics* [in Russian], Nauka, Moscow (1975).